

Inclusive production of meson resonances and the sea-quark distributions in the proton

Xie Qu-bing*

Institute of Theoretical Science, University of Oregon, Eugene, Oregon 97403

(Received 1 June 1981)

We have extended the application of the recombination model to the production of meson resonances. The x distributions of mesons produced in pp reactions, including resonances, were found to display certain simple relations, which are independent of specific assumptions about the sea-quark distributions. These predictions can be used both to examine the model and to differentiate between the distributions of strange and nonstrange sea quarks. In the smaller- x region the shapes of meson inclusive distributions sensitively depend on the sea-quark distribution. Because in the pseudoscalar-meson case that is just in the same region where contamination from the resonance decay is serious, we use resonance production to determine directly the sea-quark distributions. If we assume that the sea-quark distributions of all three flavors have the same x dependence, with only the normalization of the strange-quark distribution being suppressed, good agreement with the available data can be achieved. And, with the distribution of sea quarks known, the shape of the inclusive distribution for meson production can then be determined without any further adjustable parameters.

I. INTRODUCTION

Having discovered that the π^+ x distribution in the proton fragmentation region is very similar to that of valence quark u in the proton,¹ Das and Hwa proposed the recombination model.² In the model a pseudoscalar meson is formed by a valence quark q_1 picking up a sea quark \bar{q}_2 from the initial proton, and the inclusive distribution of meson and the distribution of sea quarks are connected intuitively. This simple model has been supported by many experimental results and people have realized more and more the function of sea quarks in high-energy reactions. But neither deep-inelastic lepton-nucleon scattering nor high-mass muon-pair experiments can give the exact sea-quark distribution for individual flavors.^{3,4} In fact the sea-quark distributions given by Field and Feynman which people usually adopt is conjectural.³ In order to get reliable information about sea quarks some authors have used the original recombination model to determine the sea-quark distribution from inclusive cross section of pseudoscalar mesons.^{5,6} But there exist two important shortcomings. First, because there are some ambiguities and arbitrariness in the original model it is difficult to discover the intrinsic relations among basic quantities and among the reactions. Second, since it is now clear that most of the pseudoscalar mesons observed in

the experiments are from resonance decay,⁷ the x distribution has substantial contribution from the decay spectra of resonances, especially in the smaller- x region. But the sea-quark distributions are concentrated in $x < 0.5$, and consequently can only affect the normalization of the distribution in the high- x region, not its shape.

Aiming at the first shortcoming, Hwa has improved the earlier model. The recombination model has been reformulated on a firm basis.⁸ In principle, it is applicable to any inclusive reaction. So far, the recombination model has not been applied to resonance production. In this paper, we apply the reformulated recombination model to inclusive production of every kind of meson including vector and tensor mesons, and then discuss quantitatively the relationship among inclusive distributions of mesons and their connection with sea quarks. We propose a way to overcome the second shortcoming by using the distribution shapes of meson resonances to determine directly the distributions of every flavor of sea quark. As a tentative step we assume that the nonstrange and strange sea quarks have the same shape of distribution, but the normalization of the latter is relatively suppressed. Thus there are only two parameters which characterize the sea-quark distributions in our approach. Appropriately choosing the two parameters, we can achieve consistency with data

now available, and determine the sea-quark distributions in the proton. Inversely, if we know them, we can predict the inclusive distribution shape of every kind of meson without parameter.

In Sec. II the new recombination model is reviewed and the possibility of application to meson resonances is studied. In Sec. III we extend the model to every kind of meson, show the x distributions, and discuss their basic behavior. In Sec. IV we determine two parameters and compare the theory with the meson resonance x distributions and pseudoscalar-meson data. In Sec. V the sea-quark distributions are given.

II. THE IMPROVED RECOMBINATION MODEL AND THE EXTENSION OF ITS APPLICATION TO RESONANCES

The recombination model assumes that the pseudoscalar mesons π, K , which are produced in the fragmentation region of the initial proton, are composed of a quark q_1 and an antiquark \bar{q}_2 which exist in the initial proton. Hence the inclusive distribution of meson M is

$$\frac{x}{\sigma} \frac{d\sigma}{dx} = f^M(x) = \int \int F^{p \rightarrow M}(x_1, x_2) R^M(x_1, x_2; x) \times \frac{dx_1}{x_1} \frac{dx_2}{x_2}, \quad (1)$$

where $F(x_1, x_2)$ is the $q_1\text{-}\bar{q}_2$ joint momentum probability distribution for the initial proton, and $R^M(x_1, x_2; x)$ is the $q_1\text{-}\bar{q}_2$ recombination function. Thus the key to improve the earlier model is to formulate F and R on a firm basis. And the priority to its further application to meson resonances is how to determine the R^M .

A. Valons and the improved recombination model

Trying to unify the two views of constituent quarks in the bound-state problem of the hadrons and the partons as probed in deep-inelastic scattering in the framework of quantum chromodynamics, Hwa has explicitly introduced the concept of valons.⁹ A valon is defined to be a dressed valence quark in QCD. Using it in context of inclusive reactions the connections between soft hadronic reactions and quarks and gluons are made clearer, and the eventual closer with QCD is helpful.

A valon is a valence quark together with its

cloud of gluons and sea quarks which can be resolved by high- Q^2 probes, and its structure function is determined by gluon bremsstrahlung and quark-pair creation in the framework of QCD. At sufficiently low Q^2 the internal structure of a valon can no longer be resolved. Let $G_{v/h}(y)$ describe the valon distribution in a hadron; it is just the uncalculable wave function of the constituent quarks. Its normalization is

$$\int_0^1 G_{v/h}(y) dy = 1 \quad (2)$$

and it satisfies the momentum sum rule

$$\int_0^1 G_{v/h}(y) y dy = \begin{cases} \frac{1}{3} & (h = \text{nucleon}) \\ \frac{1}{2} & (h = \text{nonstrange meson}) \end{cases} \quad (3)$$

We assume the simple form

$$G_{v/N}(y) = \left[B \left[\frac{k}{2}, K \right] \right]^{-1} y^{k/2-1} (1-y)^{K-1}. \quad (5)$$

Using the deep-inelastic neutrino scattering data Hwa has determined $k=3$; thus

$$G_{v/N}(y) = 6.56 y^{1/2} (1-y)^2, \quad (6)$$

and the two-valon distribution can be obtained by symmetry considerations and the sum rule

$$G_{vv/N}(y_1, y_2) = 19.9 [y_1 y_2 (1-y_1-y_2)]^{1/2}. \quad (7)$$

Similarly, the valon distribution in a nonstrange meson that satisfies Eqs. (2) and (4) is

$$G_{v/M}(y) = [B(j, j)]^{-1} [y(1-y)]^{j-1}, \quad (8)$$

and the two-valon distribution is

$$G_{vv/M}(y_1, y_2) = [B(j, j)]^{-1} (y_1 y_2)^{j-1} \delta(y_1 + y_2 - 1). \quad (9)$$

For the pion j is already determined from the massive-lepton-pair production

$$j = 1. \quad (10)$$

Hence, the valon distribution in a pion has a very simple form:

$$G_{v/\pi}(y) = 1, \quad (11)$$

$$G_{vv/\pi}(y_1, y_2) = \delta(y_1 + y_2 - 1). \quad (12)$$

Because the valon and antivalon which form the meson have evolved from quark q_1 and \bar{q}_2 , the q_1 and \bar{q}_2 can originate from any valon in the proton. They may either be from a same-flavor valon, or from a different-flavor valon. Let $K(z)$ denote the

invariant distribution of finding a quark with momentum fraction z in a valon of the same flavor, and $L(z)$ denote the unfavored distribution. Therefore, as an example, we can express the joint distribution $F^{p \rightarrow \pi^+}(x_1, x_2)$ as

$$F(x_1, x_2) = F^{(1)}(x_1, x_2) + F^{(2)}(x_1, x_2) \quad (13)$$

$$F^{(1)}(x_1, x_2) = 2 \int dy G_{U/p}(y) \frac{1}{2} \left[K \left[\frac{x_1}{y} \right] L \left[\frac{x_2}{y-x_1} \right] + L \left[\frac{x_2}{y} \right] K \left[\frac{x_1}{y-x_2} \right] \right] \\ + \int dy G_{D/p}(y) L \left[\frac{x_1}{y} \right] L \left[\frac{x_2}{y-x_1} \right], \quad (14)$$

$$F^{(2)}(x_1, x_2) = 2 \int dy_1 \int dy_2 G_{UU/p}(y_1, y_2) K \left[\frac{x_1}{y_1} \right] L \left[\frac{x_2}{y_2} \right] \\ + 2 \int dy_1 \int dy_2 G_{UD/p}(y_1, y_2) \left[K \left[\frac{x_1}{y_1} \right] + L \left[\frac{x_1}{y_1} \right] \right] L \left[\frac{x_2}{y_2} \right]. \quad (15)$$

Because the q_1 with same flavor of the valon may either be the valence quark, or from sea quarks, K can be expressed as

$$K(z) = K_{NS}(z) + L(z), \quad (16)$$

where $K_{NS}(z)$ (NS indicate nonsinglet) is determined from leptonproduction data at low Q^2 (Ref. 9):

$$K_{NS}(z) = 1.2(z)^{1.1}(1-z)^{0.16}. \quad (17)$$

The unfavored distribution $L(z)$ of course comes from the sea quark in the valon; we adopt the same canonical form:

$$L(z) = \alpha(1-z)^\beta. \quad (18)$$

The parameters α and β will be discussed later.

To distinguish $G_{U/p}(y)$ and $G_{D/p}(y)$ would require more accurate data than we now have. As in 8, we shall not in this paper be concerned with flavor dependence of $G_{v/N}$, i.e., let

$$G_{U/p} = G_{D/p} = G_{v/N}, \\ G_{UU/p} = G_{UD/p} = G_{vv/N}.$$

B. Recombination function

In the original model the recombination function is assumed to have the form

$$R(x_1, x_2; x) = \alpha_M \frac{x_1}{x} \frac{x_2}{x} \delta \left[\frac{x_1}{x} + \frac{x_2}{x} - 1 \right], \quad (19)$$

where α_M is an unknown normalization constant of order unity. The phenomenological considerations which lead to this form do not depend on whether the produced hadron is π or K .²

In the new recombination model the absolute square of the wave function $\langle V_1(y_1) V_2(y_2) | \pi \rangle$ describes not only the probability of finding the two valons of a pion at y_1 and y_2 , but also the probability of forming a pion from two valons at the same y_i values. Thus the invariant recombination function is

$$R^\pi(y_1, y_2) = F_{vv/\pi}(y_1, y_2) \\ = y_1 y_2 G_{vv/\pi}(y_1, y_2). \quad (20)$$

If we substitute (12) into (20), and note that y would change normalization from 1 into pion momentum x , then we get

$$R^\pi(x_1, x_2; x) = \frac{x_1 x_2}{x^2} \delta \left[\frac{x_1}{x} + \frac{x_2}{x} - 1 \right]. \quad (21)$$

It then reduces to (19) and $\alpha_M = 1$; this is just the result of $j=1$ in Eq. (8) for π . Thus it is not only an excellent theoretical proof of (19), but also

shows that R is not universal. But if so, we can determine the recombination function for any other meson only after we get its valon distribution from experiment. For some stable particles like p and π , we can extract its valon distribution from the deep-inelastic lepton scattering data, but we cannot do it for meson resonances.

We have first studied nonstrange meson resonances, including $\rho, \omega, f, A_1, A_2, \phi, f', \dots$. Because all their $G_{v/M}$ must satisfy the conditions (2) and (4), the simplest symmetric forms can only be of the type shown in (8) and (9); hence only the j value may be different. After substitution R 's corresponding to different j ($j \geq 1$) into Eq. (1), we determined $f^M(x)$ by numerical integration and have found both the normalization and shape are insensitive to the value of j . This important fact, i.e., that the x distribution of mesons is determined only by the distribution of q_1 and \bar{q}_2 which are in the initial proton, is just required by the recombination mechanism. For example, both π^+ and ρ^+ are composed of u and \bar{d} ; in the initial proton the x_1 and x_2 distributions of u and \bar{d} are fixed, such that π^+ and ρ^+ have the same shape of x distribution, and only their normalization may be different. Thus, in fact, we do not need to consider the valon distribution of different mesons, but use (21) as a recombination function for all mesons including resonances.

Of course, though the difference of valon distributions does not reflect on the x -distribution shape, it must be related to other properties such as the size and spin of the mesons. Here, we should mention that the meson resonances have nonzero spin or nonzero orbital angular momentum. To reflect correctly the normalization of inclusive distribution, there must exist some factors which relate to spin and orbital angular momentum in its valon distribution, otherwise the description is not complete. This is a special topic; we do not discuss it in this paper. From now on we are concerned just with the shape and ratio of x distribution.

C. The flavor dependence of sea-quark distribution

So far there is not sufficient experimental and theoretical evidence to require the distributions of

$$x\bar{u}(x) = x\bar{d}(x) = 3 \int_0^1 G_{v/N}(y) L \left[\frac{x}{y} \right] dy = \frac{32.67}{12+6\lambda} (\beta+1) \int_x^1 \sqrt{y} (1-y)^2 \left[1 - \frac{x}{y} \right]^\beta dy, \quad (25)$$

$$x\bar{s}(x) = xs(x) = \lambda x\bar{u}(x). \quad (26)$$

quiescent seas of u , d , and s to be different, but we have already had apparent experimental evidence and theoretical reasons that require an enhanced sea which saturates the momentum sum rule^{5,6,9} in low- P_T reactions, and the enhancement of the strange sea is different from that of the nonstrange sea. Thus in our work, we would rather assume first that the shapes of the three sea-quark distributions are the same, and that only the normalization of the strange sea is lower by a factor λ as compared to that of the others. This can be imagined since in the proton the quiescent sea (as probed in electroproduction) has flavor independence. Only the transition probability of $s\bar{s}$ is smaller due to its being more massive, when gluons convert into $q\bar{q}$ pairs. If it is not consistent with further experiments, it is easy to consider the flavor dependence of the x dependence of the sea.

Because the average momentum fraction carried by the valence quarks is

$$\bar{x} = 3 \int \int dx dy G_{v/N}(y) K_{NS} \left[\frac{x}{y} \right] = 0.45 \quad (22)$$

on the basis of the saturated sea we obtain as a constraint on L

$$\begin{aligned} 1 - \bar{x} &= 0.55 \\ &= 4 \int \int dx dy 3G_{v/N}(y) L \left[\frac{x}{y} \right] \\ &\quad + 2\lambda \int \int dx dy 3G_{v/N}(y) L \left[\frac{x}{y} \right] \\ &= (12 + 6\lambda) \int \int dx dy G_{v/N}(y) L \left[\frac{x}{y} \right]. \end{aligned} \quad (23)$$

Using (6) and (18), we get

$$\alpha = \frac{1.66}{12 + 6\lambda} (\beta + 1), \quad (24)$$

i.e., we only need two parameters λ and β to determine the sea-quark distributions:

III. THE SHAPE OF INCLUSIVE MESON DISTRIBUTIONS

For every meson, we can substitute Eq. (21) for the recombination function in Eq. (1) to determine the shape of $f(x)$; thus the shape difference can be determined by $F^{p \rightarrow M}(x_1, x_2)$. From the above we can divide $F^{p \rightarrow M}(x_1, x_2)$ into two terms $F^{(1)}(x_1, x_2)$ and $F^{(2)}(x_1, x_2)$. The one similar to Eq. (13) can be written as

$$F^{(1)}(x_1, x_2) = \int dy G_{v/N}(y) A(x_1, x_2; y) \quad (27)$$

expressing q_1 and \bar{q}_2 from one valon. The other one, similar to Eq. (14), can be written as

$$F^{(2)}(x_1, x_2) = \int \int dy_1 dy_2 G_{vv/N}(y_1, y_2) B \left(\frac{x_1}{y_1}, \frac{x_2}{y_2} \right) \quad (28)$$

expressing both q_1 and \bar{q}_2 from two different valons. We now discuss the mesons which are from the fragmentation of protons, and $G_{v/N}$ and $G_{vv/N}$ [in Eqs. (6) and (7)], which are just the valon distributions in the nucleon. We find that the distributions of different kinds of mesons corresponds to different quantities of K_{NS} and L included in A and B . For example, the mesons such as π^+ , ρ^+ , A_1^+ , A_2^+ , . . . , etc., are composed of quark clusters (valons) which are evolved from quarks u and \bar{d} . In the three valons of the proton, the x_2 distribution of \bar{d} can be only the sea distribution L ; the x_1 distribution of u in the two U valons can either be K_{NS} or L , but it belongs only to L in the D valon. Then

$$A(x_1, x_2, y) = \left[2K_{NS} \left[\frac{x_1}{y} \right] + 3L \left[\frac{x_1}{y} \right] \right] L \left[\frac{x_2}{y-x_1} \right], \quad (29)$$

$$B \left(\frac{x_1}{y_1}, \frac{x_2}{y_2} \right) = \left[4K_{NS} \left[\frac{x_1}{y_1} \right] + 6L \left[\frac{x_1}{y_1} \right] \right] L \left[\frac{x_2}{y_2} \right]. \quad (30)$$

By applying the same analysis for the mesons π^- , ρ^- , A_1^- , A_2^- , . . . , etc., which are composed of quark clusters developed from d , \bar{u} , we have

$$A(x_1, x_2, y) = \left[K_{NS} \left[\frac{x_1}{y} \right] + 3L \left[\frac{x_1}{y} \right] \right] L \left[\frac{x_2}{y-x_1} \right], \quad (31)$$

$$B \left(\frac{x_1}{y_1}, \frac{x_2}{y_2} \right) = \left[2K_{NS} \left[\frac{x_1}{y_1} \right] + 6L \left[\frac{x_1}{y_1} \right] \right] L \left[\frac{x_2}{y_2} \right]. \quad (32)$$

In the equation for A , the arguments x_1/y and $x_2/(y-x_1)$ describe the valon with momentum fraction y in the proton as in the case of release of q_1 and then with momentum fraction $y-x_1$ to release of \bar{q}_2 . Certainly, we should also consider the possibility that release of \bar{q}_2 is followed by q_1 instead, i.e., the possibility of x_2/y and $x_1/(y-x_2)$. That means we have to symmetrize the above arguments. When Eq. (29) is being symmetrized, it is reduced to Eq. (13). However, the symmetrization only modifies the behavior of $f(x)$ slightly in the large- x region. At this moment, we do not symmetrize A , but we list A and B for every meson in Table I, and study the fundamental properties of their x distributions. In Table I $L'(z)$ denotes particularly the invariant distribution of finding a strange quark s (or \bar{s}) with momentum fraction z in a valon; obviously, it is always an unfavored distribution in the proton.

From Table I we arrive at the following predictions. They should be more clearly examined from the resonance data.

- (i) The shape of the x distribution of each kind

TABLE I. The x -distribution shape of different kinds of mesons corresponds to different quantities of K_{NS} , L , and L' . The $A(x_1, x_2, y)$ and $B(x_1/y_1, x_2/y_2)$ in Eqs. (27) and (28) are listed for six kinds of mesons.

M	$A(x_1, x_2, y)$	$B(x_1/y_1, x_2/y_2)$
(1) π^+ , ρ^+ , A_2^+ , A_1^+ , . . .	$(2K_{NS} + 3L)L$	$(4K_{NS} + 6L)L$
(2) π^0 , ρ^0 , ω , f , A_2^0 , A_1^0 , . . .	$(\frac{3}{2}K_{NS} + 3L)L$	$(3K_{NS} + 6L)L$
(3) π^- , ρ^- , A_2^- , A_1^- , . . .	$(K_{NS} + 3L)L$	$(2K_{NS} + 6L)L$
(4) K^+ , $K^{*+}(890)$, $K^{*+}(1430)$, . . .	$(2K_{NS} + 3L)L'$	$(4K_{NS} + 6L)L'$
(5) K^- , $K^{*-}(890)$, $K^{*-}(1430)$, . . . , $\bar{K}^0(890)$, $\bar{K}^0(1430)$, . . .	$3LL'$	$4LL'$
(6) ϕ , f' , . . .	$3L'L'$	$4L'L'$

of meson included in a row in Table I should be the same, e.g., the shapes of ρ^0 , ω , f , A_2^0 , A_1^0 , g^0 , h are to be the same.

(ii) When x is comparatively small, L contributes major influence, i.e., $A \sim 3LL$, $B \sim 6LL$, and the shapes of mesons in rows 1, 2, and 3 are basically the same. When x is gradually increased, K_{NS} is more significant, than, for example, $A \sim 2K_{NS}L$ and $B \sim 4K_{NS}L$ for ρ^+ and A^+ , $A \sim K_{NS}L$ and $B \sim 2K_{NS}L$ for ρ^- and A^- ; thus

$$f\rho^+(x)/f\rho^-(x) = fA^+(x)/fA^-(x) \approx 2. \quad (33)$$

(iii) If our assumption in the previous section is true, i.e., the shape of the strange sea-quark distribution is similar to that of the nonstrange sea-quark distribution and only the normalization differs by a factor λ , then $L' = \lambda L$ and the shapes of mesons in rows 1,4 and 5,6 are exactly the same; also

$$\begin{aligned} f\rho^+(x)/fK^{*+(890)}(x) &= fA_z^+(x)/fK^{*+(1430)} \\ &= fK^{*-(890)}(x)/f\phi(x) \\ &= fK^{*-(1430)}(x)/f^1(x) \\ &= \dots = 1/\lambda. \end{aligned} \quad (34)$$

$$\begin{aligned} f^M(x) &= \frac{1}{x} \int_0^x dx_1 \left[6.56 \int_x^1 dy y^{1/2}(1-y)^2 \left\{ \left[eK_{NS} \left[\frac{x_1}{y} \right] + fL \left[\frac{x_1}{y} \right] \right] L \left[\frac{x-x_1}{y-x_1} \right] \right. \right. \\ &\quad \left. \left. + L \left[\frac{x-x_1}{y} \right] \left[qK_{NS} \left[\frac{x_1}{y-x+x_1} \right] + hL \left[\frac{x_1}{y-x+x_1} \right] \right] \right\} \right. \\ &\quad \left. + 19.9 \int_x^{1-(x-x_1)} dy_1 \int_{x-x_1}^{1-y_1} dy_2 [y_1 y_2 (1-y_1-y_2)]^{1/2} \right. \\ &\quad \left. \times \left[lK_{NS} \left[\frac{x_1}{y_1} \right] + mL \left[\frac{x_1}{y_1} \right] \right] L \left[\frac{x-x_1}{y_2} \right] \right]. \end{aligned} \quad (36)$$

Here e, f, g, \dots are various definite constants for each kind of mesons, and are listed in Table II.

It has been realized in recent years that a large fraction of pseudoscalar mesons are decay products of resonances; for example, some authors even claim the fraction of directly produced pions to be as low as 25%,¹⁰ but the major fraction of vector and tensor mesons are directly produced, and this topic has been studied in detail by this author.⁷

If the above ratios depend on x , then $L' \neq \lambda L$ and strange sea quarks have a different shape.

(iv) When $L' = \lambda L$, even if x is small, the shapes of mesons of types 5,6 fall off more rapidly in comparison with the previous four kinds.

(v) If $L' = \lambda L$, then from the ratio of the pair of either particles of types 1,4 or particles of types 5,6 we can determine λ . If $L' \neq \lambda L$, we can directly determine L' , in terms of the x distribution of particles of type 6, and then distribution $xs(x) = x\bar{s}(x)$.

(vi) In case of large x and $L' = \lambda L$:

$$\begin{aligned} fK^{*+(890)}(x)/f\rho^-(x) &= fK^{*+(1430)}(x)/fA_z^-(x) \\ &= \dots \approx 2\lambda. \end{aligned} \quad (35)$$

The first two predictions, independent of any concrete properties of K_{NS} and L , can be used to check the present theory; and the last four can be used to determine the properties of the sea-quark distribution.

IV. COMPARISON WITH DATA

Symmetrizing the $A(x_1, x_2, y)$ of Table I and substituting quantities into formula (1), we obtain explicit formulas of the x distribution of the six kinds of meson which are included in Table I:

Thus meson resonances are expected to give more direct information on the primary production mechanism than pions or kaons. And recently, the experiments have strongly suggested the possibility that a large fraction of vector mesons are produced as fragmentation products of incident particles.¹¹ Now we first determine the parameters, β , λ from the vector-meson data, and then compare the meson inclusive distribution data with theory. The

TABLE II. The values of constants $e, f, g, h, l,$ and m in Eq. (37) for each kind of meson are listed.

M	e	f	g	h	l	m
(1) $\pi^+, \rho^+, A_1^+, A_2^+ \dots$	1	2	1	1	4	6
(2) $\pi^0, \rho^0, \omega, f, A_2^0, A_1^0 \dots$	0.75	2.25	0.75	0.75	3	6
(3) $\pi^-, \rho^-, A_2^-, A_1^- \dots$	0.5	2.5	0.5	0.5	2	6
(4) $K^+, K^{*+}(890) K^{*+}(1430)$	λ	2λ	λ	λ	4λ	6λ
(5) $K^-, K^{*-}(890) \dots, \bar{K}^0, \bar{K}^{*0}(890), \dots$	0	1.5λ	0	1.5λ	0	4λ
(6) ϕ, f'	0	$3\lambda^2$	0	0	0	$4\lambda^2$

reader is reminded that the absolute normalization of our theoretical predictions is arbitrary.

At present, only ρ^0 has much data available of x distributions in high-energy reactions. Figure 1 shows the $\rho^0 x$ distributions of projectile and target fragmentation in 147-GeV/c pp reactions, and $\rho^0 x$ distribution of target-proton fragmentation in 147-

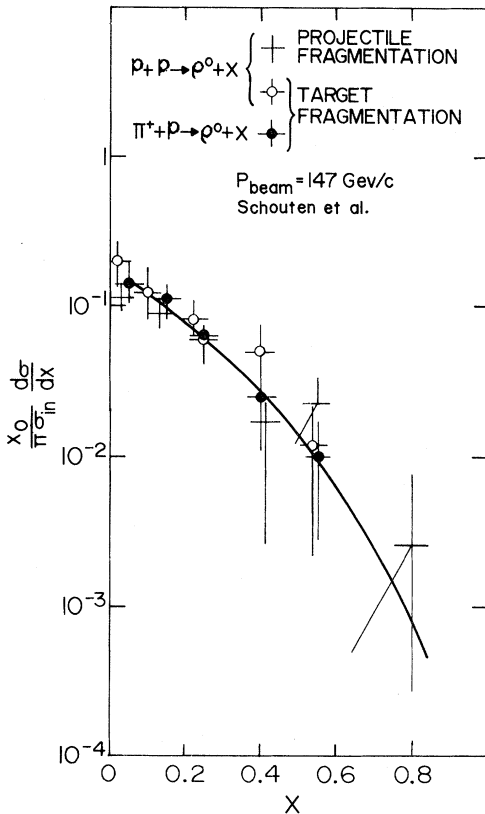


FIG. 1. The $\rho^0 x$ distributions of projectile and target fragmentation in 147-GeV/c pp reactions, and $\rho^0 x$ distribution of target-proton fragmentation in 147-GeV/c π^+p reactions. Data are from Ref. 12. To fit these data, we use $\beta=1.5$. The solid line is our theoretical curve using $\beta=1.5$.

GeV/c π^+p reactions.¹² To fit these data, we use

$$\beta=1.5. \quad (37)$$

The solid line in Fig. 1 is a theoretical curve using $\beta=1.5$.

The predictions (iii) and (v) of Sec. III can be used directly to examine whether $L'=\lambda L$ holds or not, and to determine the value of parameter λ . So far, we have not obtained those ratio data, but the experiments¹³ give the x distributions of $K^{*+}(890)$ and $\rho^0(770)$ in 24-GeV/c and 12-GeV/c pp reactions, and show that the x dependences of $K^{*+}(890)$ and ρ^0 are nearly the same; only their normalizations are different by a factor λ . Figure 2 gives the 24-GeV/c data, which has been converted into invariant distributions, and the points of ρ^0 are multiplied by $\lambda=0.18$, the ratio of the normalizations. The solid lines in the figure are theoretical curves for ρ^+ and ρ^0 , the difference between which is so small that from the data $f^{\rho^+}(x)/f^{K^{*+}(890)}(x)=1/0.18$ we can take

$$f^{\rho^+}(x)/f^{K^{*+}(890)}(x)=1/\lambda$$

and

$$\lambda=0.18. \quad (38)$$

We can see from Ref. 13 that when energy is less than 50 GeV/c λ decreases a little bit with respect to the decreasing of energy, and when the energy is large it may approach a constant. At present we do not have the data in high-energy reactions, and because the value of λ does not affect the shape of the inclusive distribution, it only affects the normalization of mesons which contain strange quarks. We assume first that $\lambda=0.18$ which does not change with respect to energy.

Figure 3 shows the comparisons between the $\rho^0, f, g^0, h, K^{*-}(890)$ data¹⁴ and our theoretical curves (solid lines). Here, the normalizations are

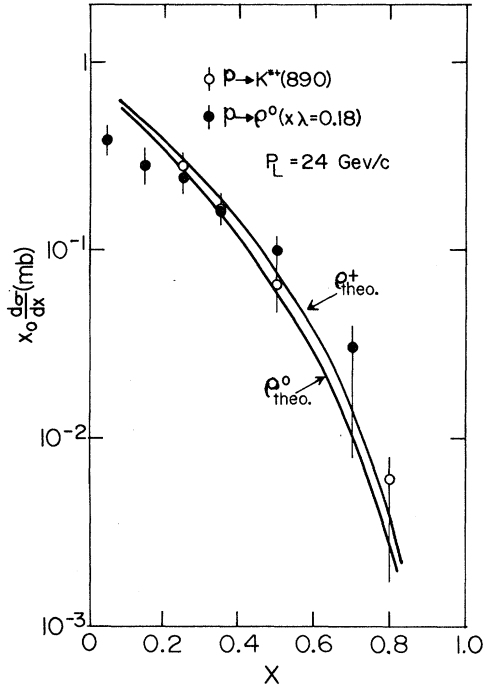


FIG. 2. The x distributions of $K^{*+}(890)$ and $\rho^0(770)$ in 24-GeV/c pp reactions (Ref. 13) have been converted into invariant distributions, and the points of ρ^0 are multiplied by $\lambda=0.18$, the ratio of normalizations. The solid lines are our theoretical curves for ρ^+ and ρ^0 .

taken arbitrarily as in the data. The curve of $K^{*-}(890)$ is normalized to the same value at the $x=0$ point of ρ^0 . Obviously, the data agree well with our predictions, i.e., the shapes of the x distribution of ρ^0 , f , g^0 , and h are the same; nevertheless, that of $K^{*-}(890)$ falls off more rapidly with x .

Figure 4 shows the comparisons between the data^{11,15} of ρ^0 and $K^{*+}(890)$ produced in the fragmentation region of the proton in K^+p interactions at 32 GeV/c and theoretical curves (solid lines). Even though the energy is rather small, the agreement is still very good.

In Figure 5 the comparison of the π^+ data¹⁶ and the theoretical curve. The agreement is excellent in both shape and normalization over the whole x range. But considering the serious contamination from resonance decay in the π spectrum, we suppose that the agreement is rather occasional.

The $f^{\pi^+}(x)/f^{K^+}(x)$ data are given in Fig. 6.^{17,18} According to the above data that showed $f^{\pi^+}(x)/f^{K^+}(x) \neq \text{const}$, and the data of $f^{\pi^-}(x)/f^{K^-}(x)$, Duke and Taylor concluded that the shape of the x distribution of the strange sea was different from that of the nonstrange sea, and

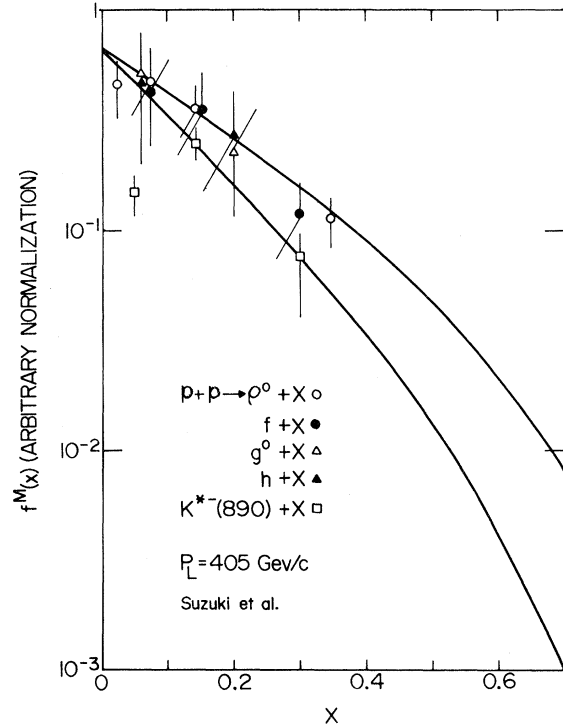


FIG. 3. The comparisons between the ρ^0 , f , g^0 , h , $K^{*-}(890)$ data (Ref. 14) and our theoretical curves (solid lines). The curve of $K^{*-}(890)$ is normalized to the same value at the $x=0$ point of ρ^0 .

chose the dashed line, as shown in Fig. 6, to determine the strange sea-quark distribution.⁵ However some of the above data should be considered as the consequence of resonance decay. In fact, even if the ratio $f^{\rho^+}(x)/f^{K^{*+}(890)}(x)$ is constant (i.e., $L'=\lambda L$), the ratio of π^+ to K^+ , that is mostly from ρ and K^{*+} , respectively, should not be constant. In the decay $K^{*+} \rightarrow K^+\pi^0$, the larger momentum is carried by K^+ ; but in $\rho^+ \rightarrow \pi^+\pi^0$ the momenta of π^+ and π^0 are the same. As a result the ratio $f^{\pi^+}(x)/f^{K^+}(x)$ increases in small x , and decreases in large x , just as shown in Fig. 5. Hence the data are not inconsistent with $L'=\lambda L$.

Figure 7 shows the comparison between the data^{17,18} of $f^{\pi^-}(x)/f^{K^-}(x)$ and the theoretical curve. In the larger- x region, the lower experimental values result from a reason similar to that mentioned above. But from Table I we can see that the yield of K^{*-} is much less than that of K^{*+} in pp reactions; the comparatively small fraction of K^- is from $K^* \rightarrow K^+\pi^-$ decay mode of nonstrange resonances (such as A_2 , f' , etc.) when compared to the case of K^+ . Consequently, the deviation between

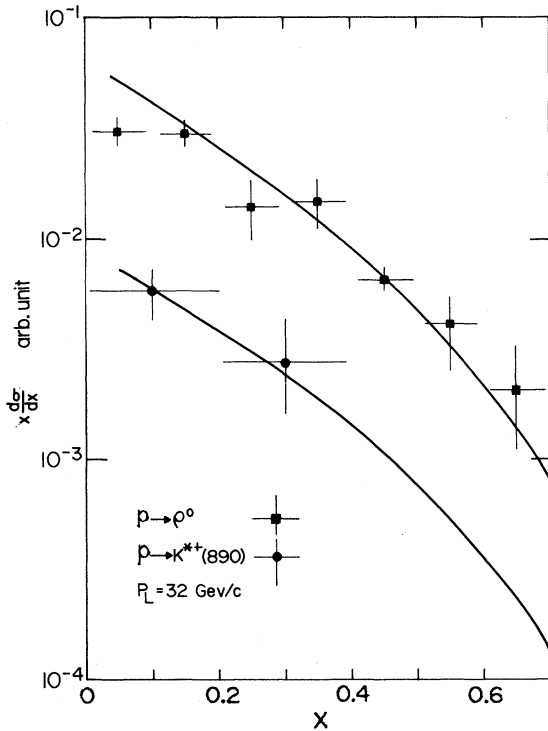


FIG. 4. The comparisons between the data of ρ^0 and $K^{*+}(890)$ produced in the fragmentation region of the proton in K^+p interactions at 32 GeV/c (Refs. 11 and 15) and our theoretical curves (solid lines).

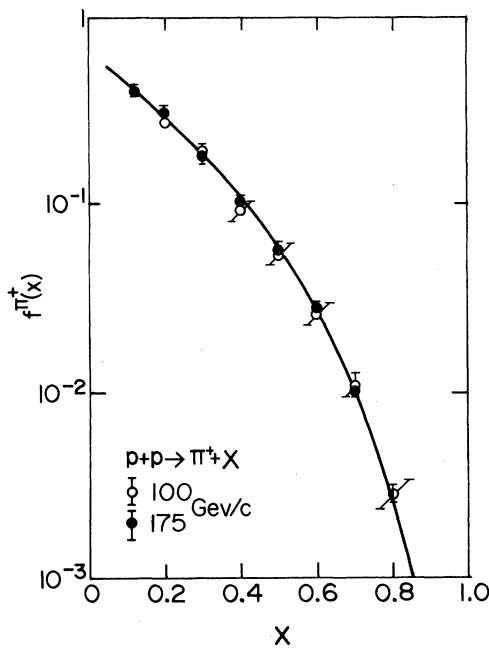


FIG. 5. The comparison of the π^+ data (Ref. 16) and the theoretical curve (solid line).

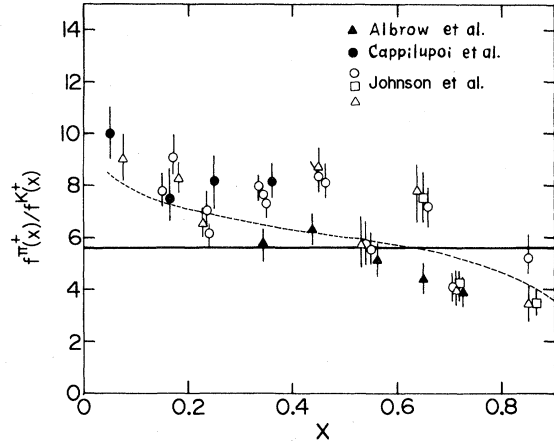


FIG. 6. The $f^{\pi^+}(x)/f^{K^+}(x)$ data versus x (Refs. 17 and 18) are shown. From the π/K ratio, Duke and Taylor concluded that the shape of the x distribution of the strange sea was different from that of nonstrange sea, and obtained the dashed line. However the above data should be considered as the consequence of resonance decay. In fact, even if the ratio $f^{\rho^+}(x)/f^{K^{*+}(890)}(x)$ is constant (solid line), in the decay $K^{*+} \rightarrow K^+\pi^0$, the larger momentum is carried by K^+ , but in $\rho^+ \rightarrow \pi^+\pi^0$ the momenta of π^+ and π^0 are the same. As a result the ratio of $f^{\pi^+}(x)/f^{K^+}(x)$ increases in small x , and decreases in large x , just as shown. Hence the data are not inconsistent with $L' = \lambda L$.

data and theory is obviously less than the ratio $f^{\pi^+}(x)/f^{K^+}(x)$.

$f^{K^+}(x)/f^{K^-}(x)$ is independent of concrete assumptions about the strange sea. In Fig. 8 one can see that the theory agrees well with data.^{17,19}

In Fig. 9 the comparison $f^{\pi^+}(x)/f^{\pi^-}(x)$ is given. According to the same reasoning as (33), when x is large, the ratio $f^{\pi^+}(x)/f^{\pi^-}(x)$ should be around 2. The dispersion of available data^{17,19} is compatible as we have predicted.

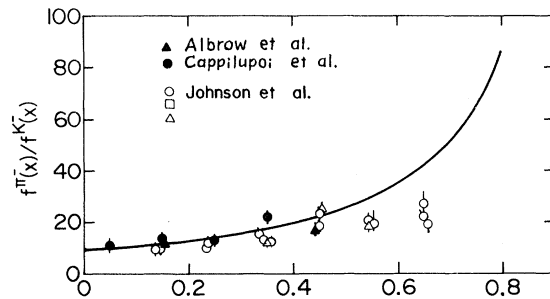


FIG. 7. The comparison between the data (Refs. 17 and 18) of $f^{\pi^-}(x)/f^{K^-}(x)$ and the theoretical curve (solid line).

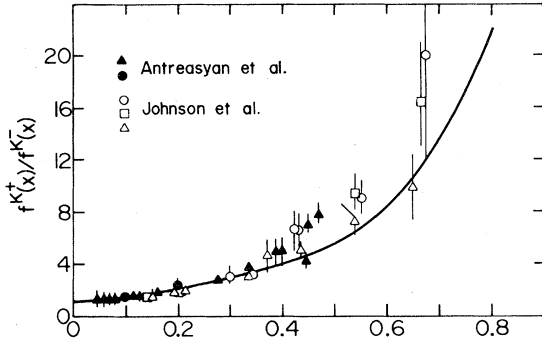


FIG. 8. The comparison between data (Refs. 17 and 19) of $f^{K^+}(x)/f^{K^-}(x)$ and the theoretical curve (solid line). This ratio is independent of concrete assumptions about the strange sea.

V. THE SEA-QUARK DISTRIBUTIONS

Using $\lambda=0.18$ and $\beta=1.5$ which have been determined in Sec. IV, we immediately obtain the nonstrange and strange sea-quark distributions from Eqs. (25) and (26):

$$\begin{aligned}
 x\bar{u}(x) &= x\bar{d}(x) \\
 &= 6.24 \int_x^1 y^{1/2}(1-y)^2 \left(1 - \frac{x}{y}\right)^{1.5} dy,
 \end{aligned}
 \tag{39}$$

$$\begin{aligned}
 xs(x) &= x\bar{s}(x) \\
 &= 1.24 \int_x^1 y^{1/2}(1-y)^2 \left(1 - \frac{x}{y}\right)^{1.5} dy.
 \end{aligned}
 \tag{40}$$

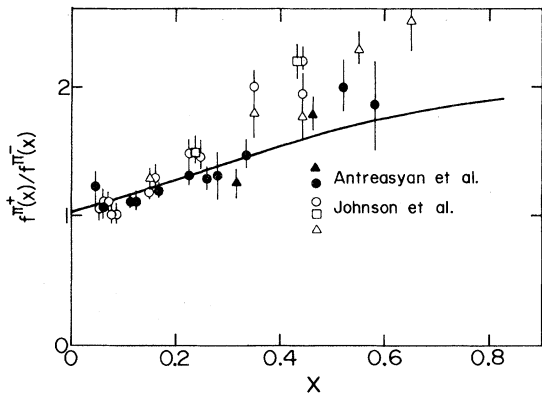


FIG. 9. The comparison between the data (Refs. 17 and 19) of $f^{\pi^+}(x)/f^{\pi^-}(x)$ and the theoretical curve (solid line).

In Fig. 10 we have plotted the distributions. They fall off more rapidly than the form $(1-x)^a$, when x is smaller, and fall off more rapidly than the form e^{-bx} , when x is larger. The distributions in the whole range can be expressed approximately as

$$\begin{aligned}
 x\bar{u}(x) &= x\bar{d}(x) \simeq 0.934e^{-5.6x}(1-x)^{2.59}, \\
 xs(x) &= x\bar{s}(x) \simeq 0.168e^{-5.6x}(1-x)^{2.59}.
 \end{aligned}
 \tag{41}$$

It is worth noting that these distributions are of the enhanced sea, which includes all of those $q\bar{q}$ pairs converted from gluons. Thus it is not certain that they have the same shape as that of the quiescent sea (as probed in electroproduction). But they directly affect the inclusive distribution and other properties of hadron-hadron reactions at high energy.

The sea-quark distributions mentioned above lead to the following fractions of momentum carried by the various quarks: valence quarks:

$$3 \int dx dy G_{v/N}(y) K_{NS} \left(\frac{x}{y} \right) = 0.450;$$

up and down sea quarks:

$$12 \int dx dy G_{v/N}(y) L \left(\frac{x}{y} \right) = 0.503;$$

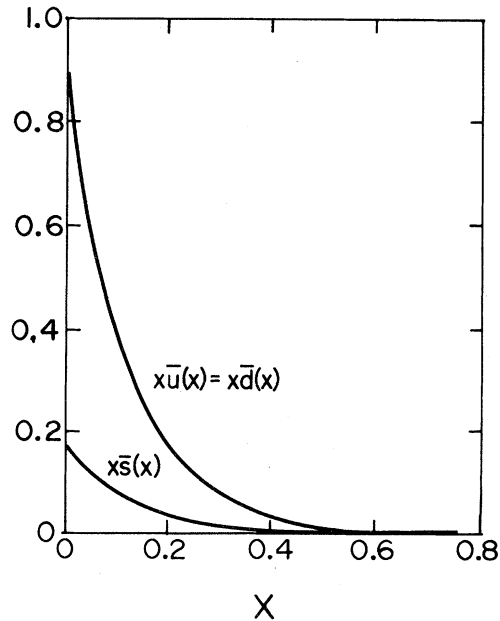


FIG. 10. The determined enhanced sea-quark distributions are plotted vs x .

strange sea quarks:

$$6\lambda \int dx dy G_{v/N}(y) L \left[\frac{x}{y} \right] = 0.045 .$$

Our results are somewhat different from those previously obtained by fitting pseudoscalar-meson data.⁵ For example, the amounts of momentum carried by the strange sea are twice the value 0.020 found in Ref. 5. But the basic behavior is similar; that is, the sea-quark distributions rapidly fall off

as x increases and are concentrated in the small- x region of $x < 0.5$.

ACKNOWLEDGMENT

The author especially thanks Professor Rudolph C. Hwa of the Institute of Theoretical Science, University of Oregon, for guidance and many very helpful discussions.

*On leave of absence from Department of Physics, Shandong University, Jinan, Shandong, People's Republic of China.

¹W. Ochs, Nucl. Phys. **B118**, 397 (1977).

²K. P. Das and R. C. Hwa, Phys. Lett. **68B**, 459 (1977).

³R. D. Field and R. P. Feynman, Phys. Rev. D **15**, 2590 (1977).

⁴J. E. Pilcher, in *Proceedings of the 1979 International Symposium on Lepton and Photon Interactions at High Energies, Fermilab*, edited by T. B. W. Kirk and H. D. I. Abarbanel (Fermilab, Batavia, Illinois, 1980), p. 185.

⁵D. W. Duke and F. E. Taylor, Phys. Rev. D **17**, 1788 (1978).

⁶N. N. Biswas *et al.*, Phys. Rev. D **19**, 1960 (1979).

⁷Xie Qu-bing, Phys. Energ. Fort. et Phys. Nucl. **4**, 439 (1980).

⁸R. C. Hwa, Phys. Rev. D **22**, 1593 (1980).

⁹R. C. Hwa, Phys. Rev. D **22**, 759 (1980).

¹⁰J. Bartke *et al.*, Nucl. Phys. B **107**, 93 (1976); G. Jansco *et al.*, *ibid.* **B124**, 1 (1977); C. Cochet *et al.*, *ibid.* **B155**, 333 (1979).

¹¹Ajinenko *et al.*, Z. Phys. C **5**, 177 (1980).

¹²M. Schouten *et al.*, Report No. HEN-187, 1981 (unpublished).

¹³K. Bockmann *et al.*, Nucl. Phys. **B166**, 284 (1980).

¹⁴A. Suzuki *et al.*, Nucl. Phys. **B172**, 327 (1980); A. Suzuki *et al.*, Lett. Nuovo Cimento **24**, 449 (1979).

¹⁵P. V. Chlapnikov *et al.*, Nucl. Phys. **B176**, 303 (1980).

¹⁶G. W. Brandenburg and V. A. Polychronakos, preliminary data of Fermilab Experiment No. E118 (see Ref. 8).

¹⁷J. R. Johnson *et al.*, Phys. Rev. D **17**, 1292 (1978).

¹⁸P. Cappiluppi *et al.*, Nucl. Phys. **B79**, 189 (1974); M. G. Albrow *et al.*, **B56**, 333 (1973); **B73**, 40 (1974).

¹⁹D. Antreasyan *et al.*, Phys. Rev. Lett. **38**, 112 (1977); **38**, 115 (1977).